



Use of ion-exchange membranes for the removal of tin from spent activating solutions

M. García-Gabaldón*, V. Pérez-Herranz, J. García-Antón, J.L. Guiñón

*Departamento de Ingeniería Química y Nuclear, Universidad Politécnica de Valencia, PO Box 22012, Valencia 46022, Spain
Tel. +34 66 175 3474; Fax: +34 96 387 7639; email: mongarga@iqn.upv.es*

Received 26 July 2008; Accepted 25 February 2009

ABSTRACT

Transport properties of tin ions through ion-exchange membranes were investigated by chronopotentiometry. Since this specie may form positively and negatively charged complex species, the present work evaluates the transport properties of tin through cation- and anion-exchange membranes. The chronopotentiometry, where a membrane potential response to an applied current density is measured, is a powerful characterization method to obtain information regarding the membrane heterogeneity, transport number of the ions through the membranes and limiting current density. Experiments developed with Sn(II) and Sn(IV) demonstrated that characteristic transition times were obtained for both cationic and anionic membranes and for a wide range of applied currents. The transition time corresponds to the moment where the interfacial salt concentration becomes zero, and it decreases as the applied current increases. A study of different NaCl concentrations revealed that chloride ions were the only species capable of crossing the anion-exchange membrane for both Sn(II) and Sn(IV) species. The behaviour of the cationic-exchange membrane was more complex and could be explained in terms of the different complex species formed between tin and chloride, and of the possible hydroxylated tin species present in the proximities of the membrane.

Keywords: Wastewater; Tin; Ion-exchange membrane; Chronopotentiometry

1. Introduction

Membrane separation techniques are becoming more and more mature for the purpose of treating effluents. Over the last years, ion-exchange membrane processes have been suggested as promising possibilities for the removal and recovery of heavy metals and other inorganic toxic substances generated in electroplating processes [1–3]. The tin present in the spent activating

solutions originated in the plastic plating industries can be recovered using an electrochemical reactor with two compartments separated by an ion-exchange membrane. In this particular case, the use of a separator is justified in order to prevent the oxidation of Sn(II) at the anode, which would lead to the loss of current efficiency in the overall process. However, the presence of a separator in an electrochemical reactor introduces an ohmic drop which contributes to the increase of the overall cell voltage. This ohmic drop has to be minimized since energy inputs and electricity costs are directly affected by the cell voltage [4].

*Corresponding author.

For the technical viability of an electromembrane process it is useful to know the electrochemical behaviour of ion-exchange membranes, their stability, conductivity, selectivity, ion transport number and the associated transport phenomena as the limiting current density. If in an electrochemical cell separated by an ion-exchange membrane the applied current exceeds the limiting current density, operational problems such as the precipitation of inorganic salts, destruction of the membrane and an increase in the energy consumption can occur, causing a decrease in the effectiveness of the process [5].

Several works have already demonstrated that chronopotentiometry, where a membrane potential response to an applied current density is measured, is a powerful characterization method to obtain information regarding the membrane heterogeneity, transport number of the ions through the membranes and limiting current density [6–18]. Compared with other characterization methods, such as impedance spectroscopy and cyclic voltammetry, it allows a direct access to the voltage contributions in different states of the membrane/solution system. Compared with steady-state voltage or current-sweeps, more detailed information can be obtained by chronopotentiometry because the dynamic voltage response in time can be analysed [7,12].

However, most of these studies have been carried out with sodium chloride solutions [6–14], and few results are presented with other ions [15–18]. In the case of the activating solutions of the electroless plating of polymers, they are mainly composed of SnCl_2 and PdCl_2 in HCl as diluting agent where tin is the major species. As a consequence of palladium reduction, and because of direct oxidation by air, Sn(II) is oxidized to Sn(IV), which may form complex species in the presence of chloride ions. On the other hand, both Sn(II) and Sn(IV) present a high tendency to form hydroxylated complex species at moderate pH values [19, 20]. Since those complex species may be positively or negatively charged, the present work evaluates the transport properties of tin through both cation- and anion-exchange membranes for a concentration range of tin similar to that occurring in the activated-wasted baths of the electroless plating of polymers.

2. Theory

When an electrical current passes through a system composed of an ion-exchange membrane separating two identical solutions, the transient process occurring near the membrane until a steady state is reached can be studied by means of chronopotentiometry, which consists on applying a current pulse and measuring the response of the potential drop across the membrane (E_m) as a function of time.

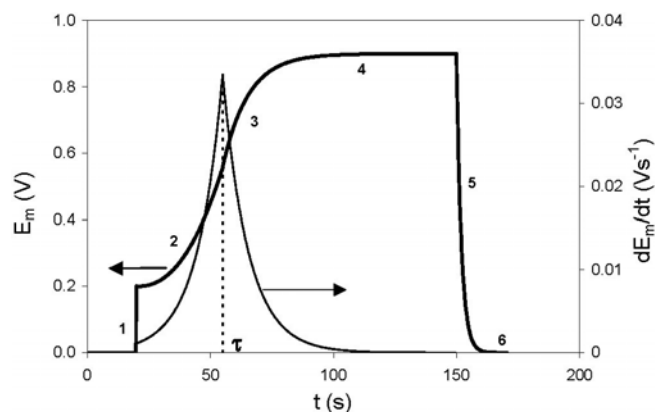


Fig. 1. Characteristic shape of a chronopotentiometric curve obtained for a current intensity above the limiting current intensity.

Fig. 1 shows a typical chronopotentiometric curve obtained at a current above the limiting current, where different regions can be defined. When a fixed current intensity is applied, after an instantaneous increase in the membrane potential (E_m) which is due to the ohmic resistance of the system (region 1 of the curve shown in Fig. 1), a slow increase in the membrane potential can be observed (region 2). When the concentration of the electrolyte drops to zero at the membrane surface, the membrane potential increases rapidly (region 3). The point at which this increase occurs is the transition time, τ , which is related with the concentration and the diffusion coefficient of the electrolyte. After the inflection point, other mechanisms of mass transfer towards the membrane surface, such as convection, become important. These mechanisms result in a decrease of the potential growth rate and its stabilization with time (region 4). The potential breakdown obtained immediately after switching-off the current (region 5) corresponds to the ohmic potential drop over the polarised membrane system. The last region, referred to as region 6, describes the diffusion relaxation of the system [7].

As mentioned above, the transition time corresponds to a sharp increase in the membrane potential drop, due to the concentration decrease in the depleting solution near the membrane/solution interface, and can be determined from the derivative of the membrane potential as a function of time as shown in Fig. 1 [3]. On the other hand, the theoretical transition time can be calculated using the Sand's equation:

$$\tau = \frac{\pi \cdot D}{4} \left(\frac{z \cdot F}{i} \right)^2 \left(\frac{C_0}{i} \right)^2 \quad (1)$$

where C_0 is the concentration of the counter-ion in the

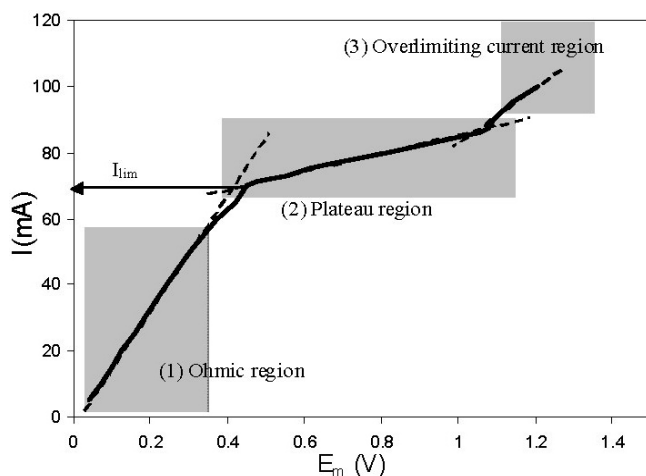


Fig. 2. Typical current-voltage curve of an ion-exchange membrane and the characteristic regions.

bulk, i is the current density, D is the electrolyte diffusion coefficient, z the charge of the counter-ion, t_i^- and t_i^+ are the transport numbers of the counter-ion in the membrane and in the solution, respectively, and F is Faraday's constant.

Typical current-voltage curves (Fig. 2) can be obtained from the constant values of the membrane potential, E_m , when the stationary state is reached in the chronopotentiograms [6,12]. In this context, three characteristic regions can be observed in the plot presented in Fig. 2: a quasi-ohmic variation of the current-voltage curves in the lower voltage range (region 1), followed by a plateau from which the value of the limiting current, I_{lim} , can be determined (region 2), and then, an increase of the current with the membrane potential (region 3). This increase is attributed to several effects: water splitting, electro-convection and the formation of space charges in the polarization layer [17]. Eq. (2) predicts a theoretical expression for the limiting current density [21]:

$$i_{lim} = \frac{z \cdot F \cdot C_0 \cdot D}{\delta(t_i^- - t_i^+)} \quad (2)$$

where δ is the diffusion boundary layer and the limiting current density, i_{lim} , is the limiting current I_{lim} divided by the membrane area (A).

3. Experimental

Chronopotentiometric curves were obtained using a two-compartment electrochemical cell as shown in Fig. 3. This cell was composed of two 250 ml symmetrical half-cells between which the ion-exchange membrane was clamped. Ionics Cation 67-HMR-412 and Ionics Anion-

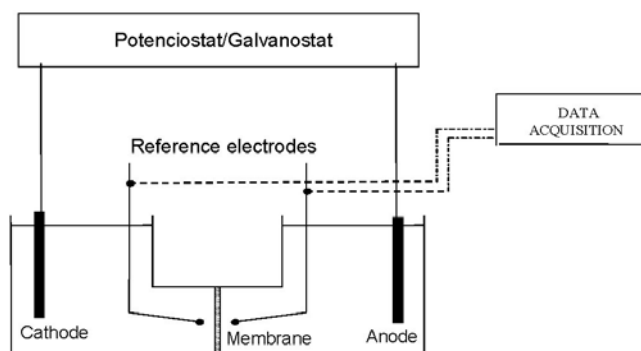


Fig. 3. Schematic diagram of the two-compartment electrochemical cell used to obtain chronopotentiometric curves.

204-SXZL-386 were used respectively as cation- and anion-exchange membranes. The main properties and characteristics of these membranes are presented in Table 1. The membrane surface area was 12.6 cm².

Two Ag/AgCl flat electrodes, obtained by anodic chlorine oxidation of silver sheets in 0.1M HCl solution, were used to impose the current in order to prevent the generation of H⁺ and OH⁻ ions by electrode reactions. Two Ag/AgCl reference electrodes immersed in Luggin capillaries were used to measure the potential drop through the membrane, E_m . The constant current was supplied by a Tacussel Electronique PJT-120-1 potentiostat/galvanostat. The membrane potential and the imposed current were registered using a PC data acquisition system. The current-voltage curves were obtained from the steady-state polarization voltage corresponding to an applied current. All experiments were conducted at room temperature and without stirring. The experiments were accomplished after a membrane equilibration period of at least 24 h using a solution with the same characteristics as that used in the experiments.

Since Sn(II) is progressively oxidized to Sn(IV) in the activating solutions, synthetic solutions of Sn(IV) and Sn(II) from analytical reagent grade SnCl₄·4H₂O and SnCl₂·2H₂O were prepared. The selected tin concentrations were similar to that occurring in the real solutions and were in the range of 10⁻²M. The applied current pulses depended on the electrolyte concentration and on the ion-exchange membrane under study.

4. Results

Fig. 4 shows a characteristic set of chronopotentiometric curves measured in the cation-exchange membrane at different applied current intensities for an electrolyte concentration of 0.01M SnCl₄. When the applied current is lower than the limiting value (120 mA), no sudden increase in the membrane potential (E_m) is

Table 1

Main properties and characteristics of the 67-HMR-412 cation-exchange membrane (CEM) and the 204-SXZL-386 anion-exchange membrane (AEM)

Properties and characteristics	CEM	AEM
Reinforcing fabric	Acrylic	Acrylic
Specific weight (mg/cm ²)	13.7	13.7
Membrane thickness (mm)	0.56–0.58	0.5
Burst strength (kg/cm ²)	7.0	7.0
Water content (% of wet resin only)	46	46
Capacity (mequiv./dry g resin)	2.10	2.20
Water transport (L per Faraday in 0.6 M NaCl; 16 mA/cm ²)	0.149	0.120

	0.01 M NaCl		0.1 M NaCl		1 M NaCl	
	CEM	AEM	CEM	AEM	CEM	AEM
Area specific resistance (ohm cm ²)	10.1	14	6	11	2	5
Specific conductance (S cm ⁻¹)	5.5×10 ⁻³	3.6×10 ⁻³	9.3×10 ⁻³	4.5×10 ⁻³	25×10 ⁻³	10×10 ⁻³
Current efficiency	0.99	0.99	0.94	0.96	0.89	0.88

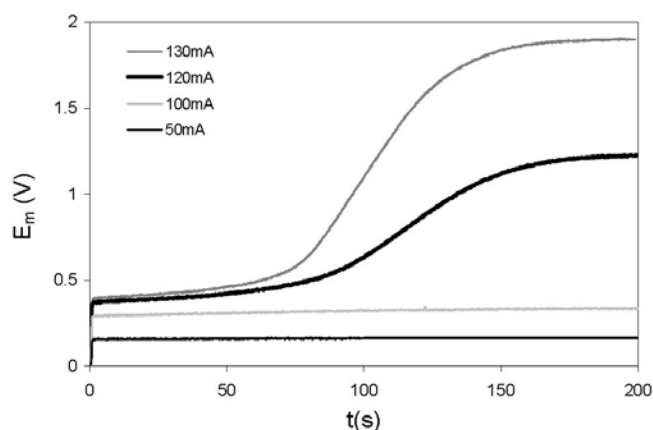


Fig. 4. Chronopotentiometric curves obtained with the cation-exchange membrane for 0.01 M SnCl₄ at different applied currents.

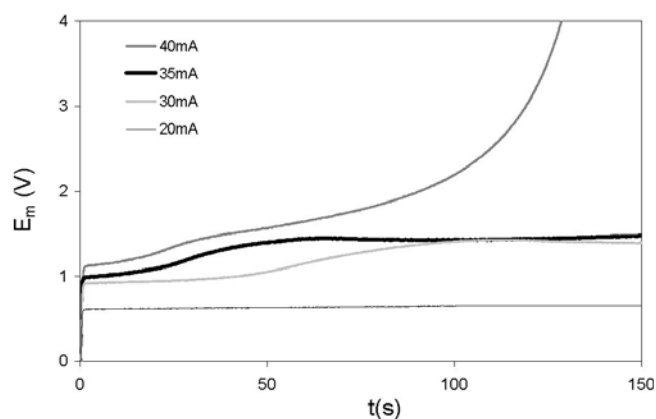


Fig. 5. Chronopotentiometric curves obtained with the cation-exchange membrane for 0.02M SnCl₂ at different applied currents.

measured in contrast to current intensities above the limiting value. Also, the curves below the limiting current are not characterized by the transition time because the concentration at the membrane solution surface does not reach a zero value. Above the limiting current, characteristic transition times are found. After the sharp membrane potential rise at the transition time, E_m levels off and a quasi-steady state is reached.

Fig. 5 presents the same representation as that shown in Fig. 4 for an electrolyte concentration of 0.02M SnCl₂. For an applied current of 20 mA no transition time is observed because the applied current is lower than the limiting value. At an applied current of 35 mA, a slight maximum in E_m is observed after the inflection point which may be attributed to the presence of protons that

are transferred through the cation-exchange membrane from the anodic compartment. These protons compete with tin cations for the transport through the membrane towards the cathodic compartment. The membrane potential decreases due to the higher mobility of the protons compared with that of Sn(II), and then a dynamic equilibrium of the H⁺/Sn(II) partition is reached within the membrane. The presence of H⁺ in solution is due to the water dissociation phenomenon occurring for over-limiting currents, generating OH⁻ and H⁺.

For applied currents higher than 35 mA, an increase of E_m is observed after a short-time plateau which coincides with the appearance of a precipitate of Sn(OH)₂ located at the anodic solution-membrane interface. The presence of this precipitate is also a consequence of the water splitting

process which takes place on cation-exchange membranes placed in divalent metallic chlorides such as SnCl_2 , MgCl_2 , NiCl_2 or CoCl_2 . In these cases, the water dissociation is promoted when the corresponding metallic hydroxides are placed under the conditions of low ionic concentration and high electrical potential [17].

Comparing Figs. 4 and 5, it is inferred that Sn(II) has a higher tendency for water dissociation in comparison with Sn(IV). On the other hand, the Sand's equation, Eq. (1), predicts that the transition time varies inversely with the applied current. This fact is reflected in both figures where the higher the applied current, the lower the transition time.

Current-voltage curves are experimentally determined by a step-wise increase of the current intensity through the cell. After an increase in the current, the system is allowed to reach a steady state for some time, after which the membrane potential is measured. The obtained combinations of current and membrane potential give the experimental current-voltage curve. An example of current-voltage curve is presented in Fig. 6 where the cation-exchange membrane behaviour for different electrolytes, 0.02 M SnCl_2 and 0.02 M SnCl_4 , is compared. The limiting current value obtained for 0.02 M SnCl_4 , around 300 mA, is higher than that obtained for 0.02 M SnCl_2 , around 25 mA.

The transport of Sn(IV) through the cation-exchange membrane is a complex phenomenon due to its high charge density leading to an important hydration shell, to its low mobility, and, particularly to its trend to form insoluble salts. On the other hand, depending on the Cl^- concentration in solution, Sn(IV) may form different charged-complex species, as shown in Fig. 7 where the speciation diagram of Sn(IV) as a function of the chloride concentration is presented.

Fig. 8 illustrates the speciation diagram of Sn(II) as a function of pH. Water splitting produces pH variations in solution due to the formation of H^+ and OH^- ions. Since

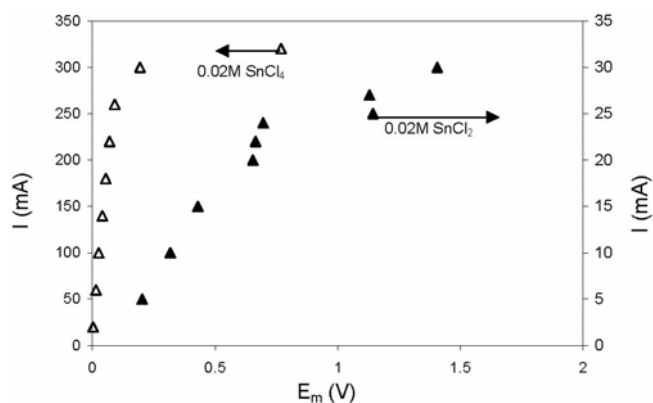


Fig. 6. Current-voltage curves of the cation-exchange membrane for 0.02 M SnCl_2 and 0.02 M SnCl_4 .

H^+ cross the membrane, OH^- ions remain in the anodic side of the cation-exchange membrane producing a local pH increase, and consequently, this fact produces the formation of positive hydroxylated complexes such as $\text{Sn}(\text{OH})^+$, which may compete for the transport through the cation-exchange membrane. Hence, the behaviour of the cation-exchange membrane is quite complex and depends on the presence of the different complex species present in solution. The lower mobility of the Sn(II) hydroxylated species in comparison with that of the Sn(IV)-Cl complexes could explain the observed behaviour in Fig. 6.

Fig. 9 presents the current-voltage curves for the anion-exchange membrane and for different electrolytes: 0.02 M SnCl_2 and 0.02 M SnCl_4 . The limiting current values observed in this figure for Sn(II) and Sn(IV) are about 35 mA and 70 mA, respectively, i.e. the limiting current of Sn(IV) is twice that of Sn(II), which means that chloride ions are the only species capable of crossing the anion-exchange membrane in both cases since the amount of chlorides liberated in solution by Sn(IV), as SnCl_4 , is two fold the amount of chlorides due to Sn(II), as SnCl_2 . This assumption is in accordance with Eq. (2) which predicts

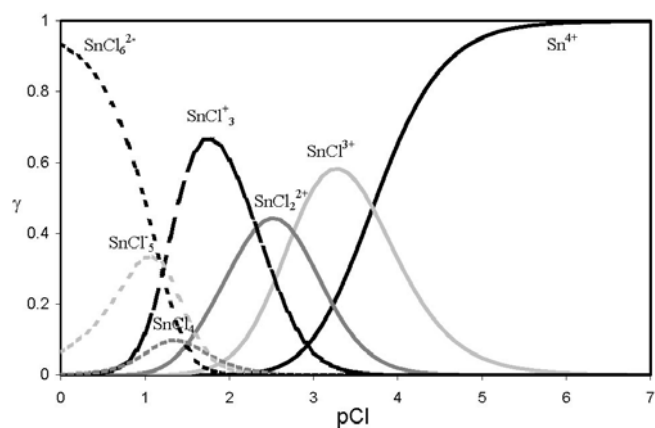


Fig. 7. Speciation diagram of Sn(IV) as a function of chloride concentration expressed as pCl.

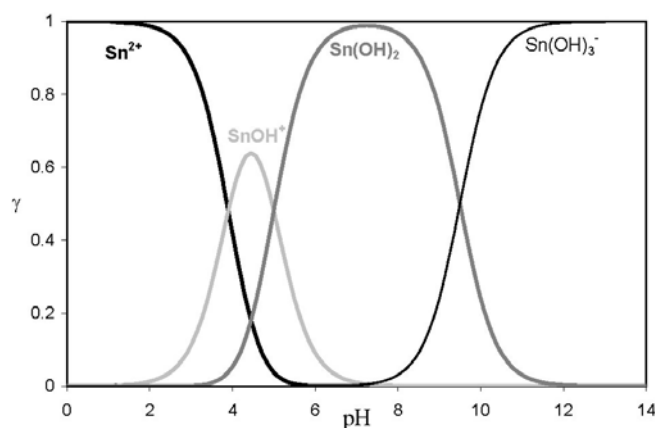


Fig. 8. Speciation diagram of Sn(II) as a function of pH.

that the limiting current depends directly on the concentration of the counter-ion in solution. This fact has important implications as the anion-exchange membrane only allows the passage of Cl^- regardless of the species under consideration, Sn(II) or Sn(IV).

In order to corroborate the previous assumption, experiments with sodium chloride in the anion-exchange membrane were carried out and are presented in Fig. 10. As observed in this figure, a similar value of the limiting current (20 mA) is obtained for 0.01 M SnCl_2 and 0.02 M NaCl since the Cl^- ions liberated in solution are the same in both cases. The same conclusion can be extrapolated for 0.02 M SnCl_2 and 0.04 M NaCl as both species have the same value of the limiting current, around 40 mA, which is twice the value obtained for 0.01 M SnCl_2 and 0.02 M NaCl. Therefore, from Fig. 10 it is inferred that Cl^- is the only species that can go through the anion-exchange membrane for both Sn(II) and Sn(IV) since the behaviour of this membrane is identical when tin is absent, as has been proved using sodium chloride.

In Fig. 10 is also observed that although the limiting current value is the same when the amount of Cl^- ions

liberated in solution is similar, such as in the case of 0.01 M SnCl_2 and 0.02 M NaCl, the membrane potential, E_m , is higher in presence of Sn(II) due to the higher mobility of Na^+ in comparison with that of Sn(II).

5. Conclusions

This work presents a study of the transport properties of two ion-exchange membranes present in an electrochemical reactor used to process the wasted and rinse baths of the electroless plating of polymers industry. These baths are composed of tin as a major species. Since tin, as Sn(II) and Sn(IV), may form positively and negatively charged complex species, this paper deals with the transport properties of tin through both cation- and anion-exchange membranes.

Chronopotentiometric experiments revealed that characteristic transition times were obtained for both cationic and anionic exchange membranes, a wide range of applied currents and electrolyte concentrations. Experiments performed in the cation-exchange membrane showed that the water splitting takes place preferably with Sn(II) rather than Sn(IV). This phenomenon could be observed by analysing the shape of the chronopotentiograms and was corroborated by the presence of a $\text{Sn}(\text{OH})_2$ precipitate in the anodic side of the cation-exchange membrane.

The current-voltage curves obtained in the cation-exchange membrane revealed that its behaviour was quite complex and depended on the presence of the different complex species present in solution which compete for the migration through the cation-exchange membrane towards the cathode: depending on the Cl^- concentration in solution, Sn(IV) may form different charged-complex species, such as SnCl^{3+} , SnCl_2^{2+} and SnCl_3^+ ; and on the other hand, the water splitting process leads to the formation of positive Sn(II) hydroxylated complex species, such as $\text{Sn}(\text{OH})^+$.

On the contrary, the transport through the anion-exchange membrane depended entirely on the chloride concentration in solution, which was corroborated by means of experiments in the presence of NaCl. The limiting current value was the same in the presence and in the absence of tin, which meant that chloride ions were the only species capable of crossing the anion-exchange membrane.

References

- [1] E. Paquay, A.-M. Clarinval, A. Delvaux, M. Degrez and H.D. Hurwitz, Applications of electrodialysis for acid pickling wastewater treatment, *Chem. Eng. J.*, 79 (2000) 197.
- [2] N. Tzanetakis, W.M. Taama, K. Scott, R.J.J. Jachuck, R.S. Slade and J. Varcoe, Comparative performance of ion-exchange membranes

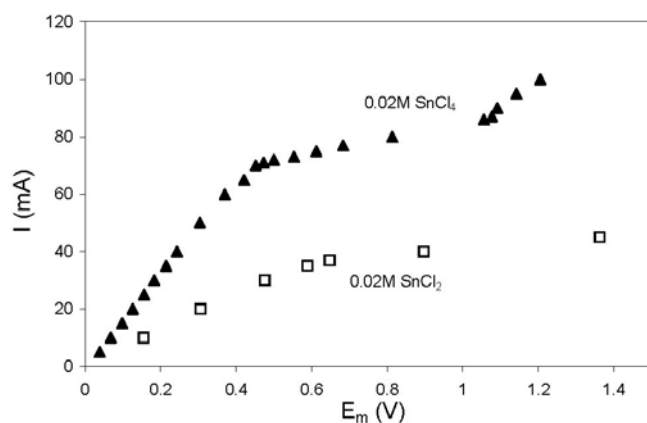


Fig. 9. Current-voltage curves of the anion-exchange membrane for 0.02 M SnCl_2 and 0.02 M SnCl_4 .

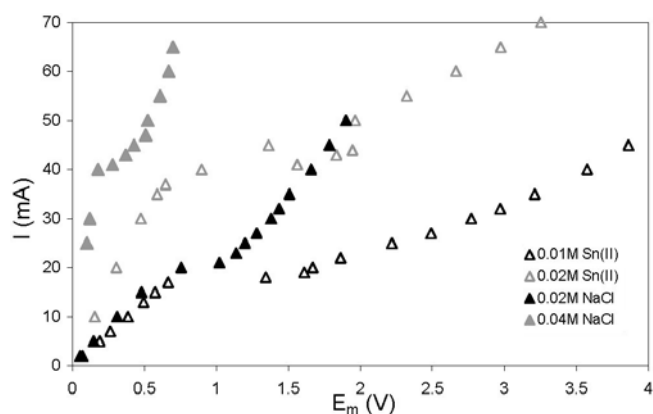


Fig. 10. Current-voltage curves of the anion-exchange membrane for different species: Sn(II), as SnCl_2 , and NaCl.

- for electro dialysis of nickel and cobalt, *Sep. Purif. Technol.*, 30 (2003) 113.
- [3] L. Marder, A.M. Bernardes and J. Zoppas Ferreira, Cadmium electroplating wastewater treatment using a laboratory-scale electro dialysis system, *Sep. Purif. Technol.*, 37 (2004) 247.
- [4] M. García-Gabaldón, V. Pérez-Herranz, E. Sánchez and S. Mestre, Effect of porosity on the effective electrical conductivity of different ceramic membranes used as separators in electrochemical reactors, *J. Membr. Sci.*, 280 (2006) 536.
- [5] Y. Tanaka, Water dissociation in ion-exchange membrane electro dialysis, *J. Membr. Sci.*, 203 (2002) 227.
- [6] R. Ibanez, D.F. Stamatialis and M. Wessling, Role of membrane surface in concentration polarization at cation-exchange membranes, *J. Membr. Sci.*, 239 (2004) 119.
- [7] N. Pismenskaia, P. Sizat, P. Huguet, V. Nikonenko and G. Pourcelly, Chronopotentiometry applied to the study of ion transfer through anion-exchange membranes, *J. Membr. Sci.*, 228 (2004) 65.
- [8] J.J. Krol, M. Wessling and H. Strathmann, Chronopotentiometry and over-limiting ion transport through monopolar ion-exchange membranes, *J. Membr. Sci.*, 162 (1999) 155.
- [9] E. Volodina, N. Pimenskaya, V. Nikonenko, C. Larchet and G. Pourcelly, Ion-transfer across ion-exchange membranes with homogenous and heterogeneous surfaces, *J. Colloid Interf. Sci.*, 285 (2005) 247.
- [10] R.K. Nagarale, V.K. Shahi, S.K. Thampy and R. Rangarajan, Studies on electrochemical characterization of polycarbonate and polysulfone-based heterogeneous cation-exchange membranes, *React. Funct. Polym.*, 61 (2004) 131.
- [11] P.V. Vyas, P. Ray, S.K. Adhikary, B.G. Shah and R. Rangarajan, Studies of the effect of variation of blend ratio permselectivity and heterogeneity of ion-exchange membranes, *J. Colloid Interf. Sci.*, 257 (2003) 127.
- [12] F.G. Wilhem, N.F.A. van der Vegt, M. Wessling and H. Strathmann, Chronopotentiometry for the advanced current-voltage characterization of bipolar membranes, *J. Electroanal. Chem.*, 502 (2001) 152.
- [13] P. Sizat and G. Pourcelly, Chronopotentiometric response of an ion-exchange membrane in the underlimiting current-range. Transport phenomena within the diffusion layers, *J. Membr. Sci.*, 123 (1997) 121.
- [14] J.-H. Choi, S.-H. Kim and S.-H. Moon, Heterogeneity of ion-exchange membranes: the effects of membrane heterogeneity on transport properties, *J. Colloid Interf. Sci.*, 241 (2001) 120.
- [15] J.-H. Choi and S.-H. Moon, Pore-size characterization of cation-exchange membranes by chronopotentiometry using homologous amine ions, *J. Membr. Sci.*, 191 (2001) 225.
- [16] H.-W. Rösler, F. Maletzki and E. Staude, Ion transfer across electro dialysis membranes in the over-limiting current range: chronopotentiometric studies, *J. Membr. Sci.*, 72 (1992) 171.
- [17] M. Taky, G. Pourcelly, C. Gavach and A. Elmidaoui., Chronopotentiometric response of a cation-exchange membrane in contact with chromium (III) solutions, *Desalination*, 105 (1996) 219.
- [18] P. Ray, V.K. Shahi, T.V. Pathak and G. Ramachandraiah, Transport phenomena as a function of counter and co-ions in solution: chronopotentiometric behaviour of anion exchange membrane in different aqueous electrolyte solutions, *J. Membr. Sci.*, 160 (1999) 243.
- [19] P. Kiekens, H. Verplaetse, H. Donche and E. Temmerman, Kinetic behaviour of the Sn(IV)-Sn(II) couple in acidified concentrated bromide solutions at a glassy carbon rotating-ring disk electrode, *Electrochim. Acta*, 27 (1982) 623.
- [20] N. Fatouros and M. Chemla, Electrochemical kinetics of the Sn(II)-Sn(IV) couple in aqueous HCl solution. Electronic charge-transfer coupled to a chemical reaction, *J. Chim. Phys. Physico-Chim. Biol.*, 78 (1981) 647.
- [21] J.J. Krol, M. Wessling and H. Strathmann, Concentration polarization with monopolar ion-exchange membranes: current-voltage curves and water dissociation, *J. Membr. Sci.*, 162 (1999) 145.